Determining gap nodal structures in Fe-based superconductors: angle-dependence of the low temperature specific heat in an applied magnetic field

S. Graser,[1] G.R. Boyd,[1] Chao Cao,[1,2] Hai-Ping Cheng,[1,2] P. J. Hirschfeld,[1] and D. J. Scalapino[3]

[1]*Department of Physics, University of Florida, Gainesville, FL 32611, U.S.A.*[*]
[2]*Quantum Theory Project, University of Florida, Gainesville, FL 32611, U.S.A.*
[3]*Department of Physics, University of California, Santa Barbara, CA 93106-9530 USA*

(Dated: April 6, 2008)

Since the discovery of high-T_c $LaO_{1-x}F_xFeAs$ and other such systems based on FeAs layers, several proposals have been made for the superconducting order parameter $\Delta_{\mathbf{k}}$, on both phenomenological and microscopic grounds. Here we discuss how the symmetry of $\Delta_{\mathbf{k}}$ in the bulk can be determined, assuming that single crystals will soon be available. We suggest that a measurement of the dependence of the low temperature specific heat on the angle of a magnetic field in the FeAs plane is the simplest such method, and calculate representative specific heat vs. field angle oscillations for the various candidate states, using a phenomenological band structure fitted to the DFT Fermi surface.

PACS numbers: 74.70.-b,74.25.Ha,74.25.Jb,74.25.Kc

The recent discovery of superconductivity with onset temperature of 26K in $LaO_{1-x}F_xFeAs$ [1] was followed rapidly by the development of materials with T_c up to $\sim$50K[2–10], which possess a similar structure but where La has been replaced by Sm, Pr, Nd or Ce. Common to all such materials is an electronically layered structure, where according to electronic structure theories a rare-earth oxide layer where F substitutions for O dope an FeAs layer. The iron atoms are arranged in a simple square lattice, separated by arsenic atoms above and below this plane. The FeAs complex provides the bands at the Fermi level, and the Fermi surface consists of sheets around the Γ point and the M point of the Brillouin zone[11–16].

Beyond this general initial consensus on the commonalities of the different materials, electronic structure calculations differ on the details of the ground state and the band structure near the Fermi level. Both paramagnetic and antiferromagnetic (sublattice and linear SDW) ground states have been reported, with some authors claiming that the system is close to a Mott transition and also possibly to a ferromagnetic state. Crude support for the proximity of competing magnetic states is provided by the known helimagnetism in the layered iron monoarsenide system.

Within weeks of the discovery of the $LaO_{1-x}F_xFeAs$ systems, theoretical analyses of various possibilities for the mechanism of superconductivity and the symmetry of the superconducting order parameter have appeared[12, 13, 17–19]. Eliashberg style calculations based on density functional theory (DFT) determination of electron-phonon coupling constants[20] suggest that conventional electron-phonon interactions are not sufficient to generate the observed transition temperatures. Thus several authors have discussed electronic pairing mechanisms of the spin fluctuation type[12, 13, 17–19], but disagree about the symmetry of the ground state, apparently because of the details of the electronic structure used as an input to the calculation. Given the past history of theoretical approaches to unconventional superconductors, it may be some time before a consensus on the correct microscopic approach is forged.

In the intervening period, it would clearly be useful to have some information on the symmetry of the order parameter to guide such theoretical discussions. Evidence for nodes in the order parameter has already been provided by point contact tunnelling[21], which has reported a zero bias state in a series of relatively high-transparency junctions, and specific heat measurements in a magnetic field H[22], which indicate a $C_V/T \sim \sqrt{H}$ term similar to that predicted by Volovik for a d-wave (or, more generally, nodal) superconductor. Because the current experiments have been performed on powdered samples, however, the distribution on the Fermi surface of order parameter nodes, which could provide some information on the symmetry of the pair state is not yet determined. In addition, the point contact measurements probe only the superconducting state at the surface, whereas ideally one would prefer to extract information on the bulk superconducting state. When single crystals are produced, it will be possible to perform what is possibly the simplest bulk probe of the distribution of gap nodes, a measurement of the specific heat of a sample in the presence of a field in the FeAs plane as a function of its angle relative to the crystal axes. The superflow field in the vortex state of the type-II superconductor is known to "Doppler shift" the energies of quasiparticles, changing their local occupation and giving rise to a residual density of states[23] which depends on the angle the field makes with the nodes[24, 25]. This method of "nodal mapping" was proposed in the context of the cuprates, where the experiment is difficult due to the large phonon background, but has found more fruitful application in lower-T_c materials[26].

In this paper we calculate the specific heat oscillations with magnetic field angle to be expected in the presence of a variety of candidate superconducting pair states. Rather than tie ourselves to any particular microscopic electronic structure calculation, we use a phenomenological two-band model [27] which captures the essential qualitative features of the bands near the Fermi surface. We find that various extended-s like

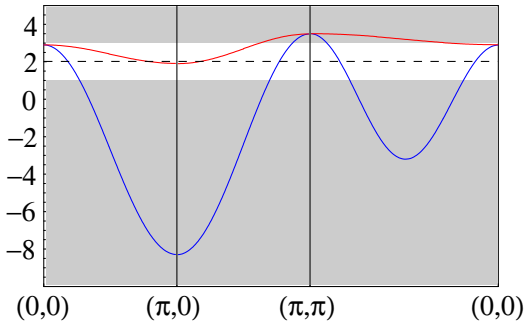

FIG. 1: (Color online) The two hybridized bands of our model. The white region depicts the narrow energy window around the Fermi energy (dashed line) where the model reproduces the semiquantitative aspects of the LDA band structure. The momenta refer to points in the 2D effective large Brillouin zone (see Fig. 2).

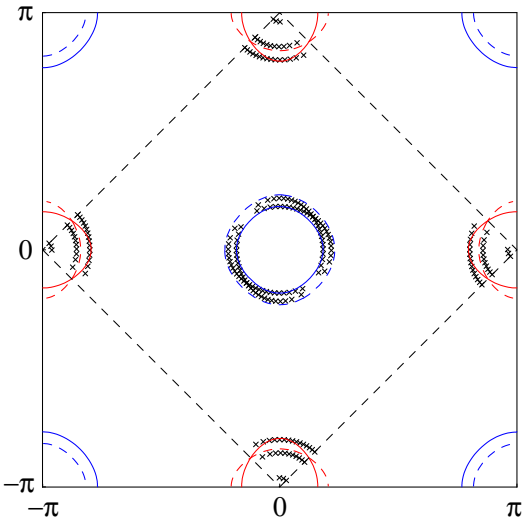

FIG. 2: (Color online) The different FS sheets in the large effective BZ calculated within our two-band model. The two hybridized bands result in two sets of Fermi surface sheets, centered around the Γ point (blue) and the M point (red) of the real BZ (dashed black line). Backfolding of the large into the small BZ produces the dashed sheets in the small zone. The black crosses show the FS of the paramagnetic ground state determined by DFT [14].

states can be distinguished from, e.g. d-wave or p-wave like states by the positions of their nodes. There are also cases, however, where nodes lie in positions on the Fermi surface where $\mathbf{k}_n$ and the Fermi velocity $\mathbf{v}_F$ are not parallel. In this case the minimum of the specific heat does not correspond precisely to the nodal position and the structure of the set of minima must be examined in detail.

Effective band structure. The crystal structure of LaOFeAs consists of alternating layers of FeAs and LaO. Density functional theory (DFT) calculations show that the energy bands crossing the Fermi level can be assigned to the Fe $3d$ and the As $4p$-orbitals [11–17]. Thus, to describe superconducting properties we can consider the LaO layers mainly as spacing layers and possible charge reservoirs. The FeAs layers can be further subdivided into a square Fe lattice with an Fe-Fe spacing $d_{Fe-Fe} = 2.82$ Å and an As square lattice displaced by a vector $(1/2, 1/2)$ in the x-y-plane to a position in the center of the Fe squares. Additionally, the As atoms are displaced alternately above or below the Fe plane leading to a pyramidal Fe-As configuration. Due to the alternating sign of the As z-displacements the primitive unit cell of LaOFeAs contains two Fe and two As atoms. The axes of the corresponding Brillouin zone (BZ) are aligned in the next nearest neighbor Fe-Fe direction and the BZ has a size of $2\pi/a \times 2\pi/a$. However, due to the high degeneracy of the two As positions we will treat an effective model consisting of a smaller unit cell having only one Fe and one As atom. This leads to a larger effective BZ that has axes that are aligned to the nearest neighbor Fe-Fe direction. In this case the *real* BZ occupies a diamond shaped region within the *effective* BZ.

Since the thermodynamic properties of the superconducting state are governed by low lying quasiparticle excitations, we restrict our considerations in the following to the region where the energy bands cross the Fermi level, forming the different Fermi surface sheets in the BZ. To simplify the rather complicated band structure, we use a two band model that takes only the iron d_{xz} and d_{yz} orbitals into account [27]. Here the basic symmetry of the hopping parameters is determined from the direct overlap of the Fe d orbitals as well as from the hopping mediated by the As p orbitals. The model neglects contributions from other orbitals, e.g. hybridization due to the other Fe d orbitals, and the hopping parameters are adjusted to give the generic form of the Fermi surface sheets determined by bandstructure calculations.

Calculating the hopping from the direct overlap of the Fe d_{xz} and d_{yz} orbitals as well as the effective hopping in second order perturbation theory on the path Fe-As-Fe, taking the As p_x, p_y and p_z into account, leads to a tight binding Hamiltonian with nearest and next-nearest neighbor hopping between the same orbitals and a next-nearest neighbor exchange hopping between the two bands. Due to the choice of the orbitals there are different nearest neighbor hopping values t_1 and t_2 for hopping in the x and y directions in one band which are interchanged in the other band. The intraband next nearest neighbor hopping t_3 is the same for both bands and both directions, while the interband hopping t_4 has a different sign for the $(1,1)$ compared to the $(1,-1)$ direction. After the usual Fourier transformation we can write the intraband energies in momentum space as

$$\epsilon_{11} = -2t_1 \cos k_x - 2t_2 \cos k_y - 4t_3 \cos k_x \cos k_y \quad (1)$$

$$\epsilon_{22} = -2t_2 \cos k_x - 2t_1 \cos k_y - 4t_3 \cos k_x \cos k_y \quad (2)$$

and the interband exchange energy is

$$\epsilon_{12} = \epsilon_{21} = -4t_4 \sin k_x \sin k_y \quad (3)$$

Taking the hybridization of the two bands into account one

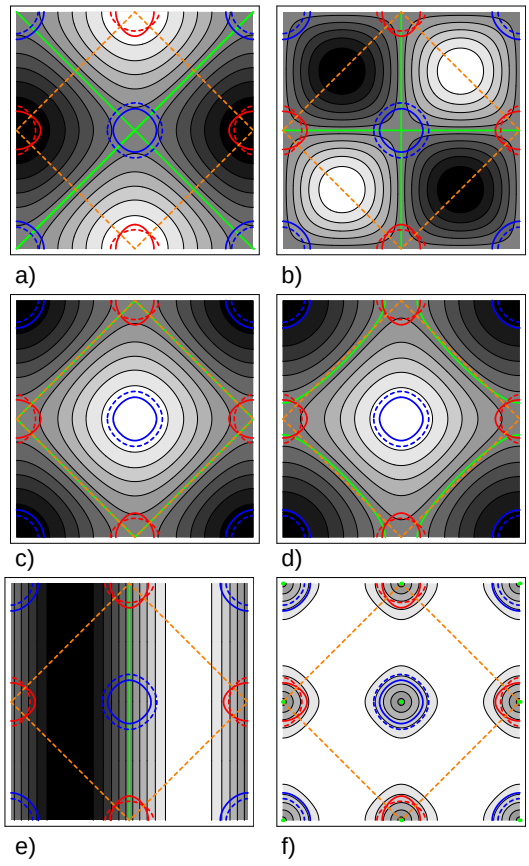

FIG. 3: (Color online) Candidate order parameter states considered in this work. a) $d_{x^2-y^2}$ state; b) d_{xy} state; c) extended-s state from Ref. [13] ; d) generalized extended-s; e) p_x state ($\Delta_{\mathbf{k}} \propto \sin k_x$); f) $p_x + ip_y$ state ($\Delta_{\mathbf{k}} = \sin k_x + i \sin k_y$) [12]. The dashed orange line denotes the small Brillouin zone and the green line denotes locus of gap nodes.

finds for the two bands

$$\epsilon^{\alpha} = \frac{1}{2}\left(\epsilon_{11}+\epsilon_{22}-\sqrt{(\epsilon_{11}-\epsilon_{22})^2+4\epsilon_{12}^2}\right) \quad (4)$$

$$\epsilon^{\beta} = \frac{1}{2}\left(\epsilon_{11}+\epsilon_{22}+\sqrt{(\epsilon_{11}-\epsilon_{22})^2+4\epsilon_{12}^2}\right) \quad (5)$$

The hopping parameters t_i and the chemical potential E_F can be used to fit the FS of the paramagnetic ground state found within the DFT calculations [14]. We find a reasonable agreement of the FS for the following values $t_1 = -1.2$, $t_2 = 1.35$, $t_3 = -0.8$, $t_4 = -0.8$ and $E_F = 2$. These values lead to the bandstructure shown in Fig. 1.

Order parameters. Because of the small coherence length of $\mathcal{O}$(30 Å), these systems are strongly type-II and it may be appropriate to think of the range of the pairing interaction as being very short, of order the lattice spacing. Generally speaking, order parameters involving pairing on nearest neighbor sites are also those which have been proposed for these systems. We therefore consider as representative candidates the states listed in Fig. 3, proposed by various authors, beginning with nearest-neighbor a) $d_{x^2-y^2}$ state ($\Delta_{\mathbf{k}} \propto \cos k_x - \cos k_y$)[19] ; b) d_{xy} state ($\Delta_{\mathbf{k}} \propto \sin k_x \sin k_y$); and c) extended s-wave state ($\Delta_{\mathbf{k}} \propto \cos k_x + \cos k_y$) [13], and e) a p_x-wave state. The extended s-wave state shown in c) changes sign on the Fermi surface of the model system, as seen in the Figure. On the other hand, its nodes are located at the 45° directions relative to the sheet center at the M point, which is not generic for a state with s (A_{1g}) symmetry. We therefore show in Fig. 3d) the result of adding to this state a higher order s-harmonic $\Delta_{\mathbf{k}} \propto (1-\gamma)(\cos k_x + \cos k_y) + \gamma(\cos 2k_x + \cos 2k_y)$ with $\gamma = 0.05$. For example, the RPA spin fluctuation calculations of Kuroki et al. appear to lead to a more general extended s-wave state. Similarly, it can be seen in Fig. 3d) that the points where the nodes cross the Fermi surface sheets are away from the 45° directions (relative to the center of the sheet on the zone face). Finally, we show in Fig. 3f) the nodeless $p_x + ip_y$ state proposed by Xu et al. [12].

Specific heat. To get a qualitative understanding of the specific heat oscillations as a function of the rotation angle of an in-plane magnetic field at low temperature it is sufficient to study the spectrum of low energy excitations. To calculate the spectrum in the vortex state we want to follow a semiclassical approach, that neglects the core states and considers only the shift of the quasiparticle energies of the extended nodal states in the presence of a magnetic field. Following [25] we approximate the vortex lattice using a circular unit cell with radius R and winding angle β. Then the Doppler shifted quasiparticle energy is

$$\delta E^{(i)} = m\mathbf{v}_F^{(i)}\mathbf{v}_s = \frac{E_H}{\rho}\left(\hat{v}_{F,y}^{(i)}\cos\alpha - \hat{v}_{F,x}^{(i)}\sin\alpha\right)\sin\beta \quad (6)$$

Here $\mathbf{v}_F^{(i)}$ denotes the Fermi velocity on band i, $\mathbf{v}_s$ is the gauge invariant expression of the quasiparticle flow field around the vortex core and α is the angle between the magnetic field and the x-axis of our coordinate system. The dimensionless radial variable $\rho = r/R$ and $\hat{v}_{F,x/y}^{(i)}$ are the components of the Fermi velocity calculated from $\nabla\epsilon_k^{(i)}$, normalized by a Fermi surface averaged value of $v_F^{(i)}$. The energy scale E_H associated with the Doppler shift is

$$E_H^{(i)} = \frac{a}{2}\tilde{v}_F^{(i)}\sqrt{\pi H/\Phi_0} \quad (7)$$

where a is a geometric constant characteristic of the vortex lattice, Φ_0 is the flux quantum, and $\tilde{v}_F^{(i)}$ is an averaged Fermi velocity on band i determined from DFT calculations. This procedure of normalizing the Fermi velocities prevents us from overestimating the differences in the energy gradients at the Fermi level of the simplified two-band model. Using the Doppler shifted energy in a BCS-like density of states we can calculate the low energy spectrum as

$$N_0^{(i)} = \mathrm{Re}\left\langle\left\langle \frac{|\delta E^{(i)}|}{\sqrt{\left(\delta E^{(i)}\right)^2 - \left(\Delta_k/E_H^{(i)}\right)^2\rho^2}}\right\rangle_H\right\rangle_{FS} \quad (8)$$

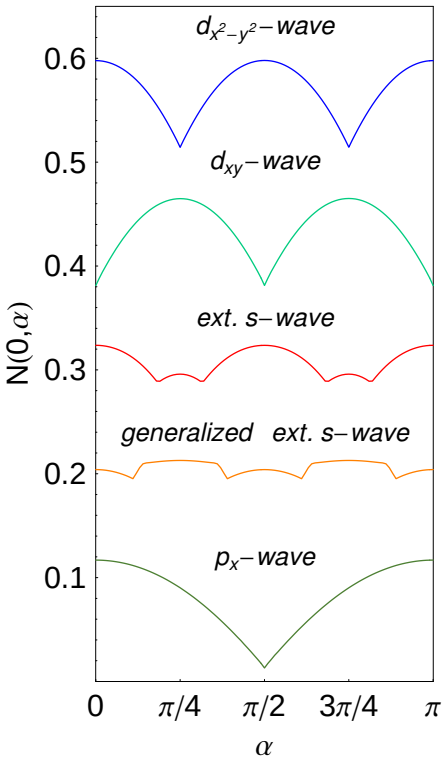

FIG. 4: (Color online) Residual density of states $N(\omega = 0, \mathbf{H})$ vs. α, the angle $\mathbf{H}$ makes with the x-axis for the different superconducting states shown in Fig. 3. $N(\omega = 0, \mathbf{H})$ is proportional to the linear specific heat coefficient at low temperature. Note all curves have been offset by a constant amount for clarity.

where the angular brackets denote an average over the vortex cell (H) and over the Fermi surface (FS), respectively. The integral over the vortex cell can be done analytically leading to

$$N_0^{(i)}(\alpha) = \left\langle \min\left[1, (E_H^{(i)}/\Delta_k)^2 \left(\hat{v}_{F,y}^{(i)} \cos\alpha - \hat{v}_{F,x}^{(i)} \sin\alpha\right)^2\right]\right\rangle_{FS} \quad (9)$$

The last average is to be performed over the different Fermi surface sheets in the unfolded Brillouin zone leading to an oscillation of the low energy spectrum as a function of the angle of the applied magnetic field. These oscillations can be directly determined by low temperature thermodynamic measurements, like specific heat or the thermal conductivity.

In Fig. 4, we show the residual angle-dependent density of states, or linear specific heat coefficient as a function of field angle θ. For the most part, one expects fairly straightforward generalizations of the results for a circular Fermi surface[25], as seen for the p_x and d-symmetry states: minima in the specific heat at low temperatures $T \ll E_H^{(i)}$ lie at the expected nodal positions. The nodeless $p_x + ip_y$ state produces no Volovik effect, is therefore not plotted in Fig. 4 and is apparently not a candidate for the Fe-based materials. In the extended-s cases, some interesting points arise. It is seen from Fig. 3c) that in the simple extended-s case, the nodes are located along the 45° directions. Nevertheless the minima in Fig. 4 are slightly displaced symmetrically with respect to these nodes; this is due to the fact that the M sheets are elliptical, with the consequence that the Fermi velocities are not parallel to nodal $\mathbf{k}_n$ measured from the sheet center. When there are higher harmonics, such as in the generalized extended s-wave case, the nodes themselves actually are displaced from the 45° directions. Thus a measurement of this kind can identify an extended s state by the displacements of the minima, but a direct correspondence with the nodal positions requires a precise knowledge of the underlying Fermi surface.

Conclusions. In this paper, we have proposed that the measurement of specific heat oscillations as a function of the magnetic field angle in the FeAs plane of the new iron-based superconductors could be the simplest and most straightforward bulk determination of gap symmetry, once single crystals or highly oriented powders are available. To simplify the calculation, we used an effective two-band model with parameters chosen to reproduce the DFT Fermi surface. We then calculated the low-temperature linear term in the specific heat to be expected as a function of field angle for a variety of candidate states. The elliptical Fermi surface pockets near the M points introduce some interesting complications in the problem relative to the usual picture of $C_V(\mathbf{H})$ oscillations over the field angle.

This work is supported by DOE DE-FG02-02ER45995, NSF/DMR/ITR-0218957 (HPC and CC), and DOE DE-FG02-05ER46236 (PJH). SG gratefully acknowledges support by the Deutsche Forschungsgemeinschaft. DJS acknowledges support from the Center for Nanophase Material Science, ORNL.

* Corresponding author, e-mail: graser@phys.ufl.edu

[1] Y. Kamihara, T. Watanabe, M. Hirano, and H. Hosono, J. Am. Chem. Soc. **130**, 3296 (2008).
[2] G. F. Chen *et al*, arXiv:0803.0128.
[3] H. Yang *et al*, arXiv:0803.0623.
[4] G. Mu *et al*, arXiv:0803.0928; X. Zhu *et al*, arXiv:0803.1288.
[5] A.S. Sefat *et al*, arXiv:0803.2528.
[6] H.H. Wen *et al*, Europhys. Lett. **82**, 17009 (2008); arXiv:0803.3021.
[7] Z. Li *et al*, arXiv:0803.2572.
[8] J. Dong *et al*, arXiv:0803.3426.
[9] L. Fang *et al*, arXiv:0803.3978.
[10] X.H. Chen *et al*, arXiv:0803.3603.
[11] D.J. Singh and M.H. Du, arXiv:0803.0429.
[12] G. Xu *et al*, arXiv:0803.1282.
[13] I.I. Mazin, D.J Singh, M.D. Johannes, and M.H. Du, arXiv:0803.2740.
[14] C. Cao, P. J. Hirschfeld, and H.-P. Cheng, arXiv:0803.3236.
[15] F. Ma and Z.Y. Lu, arXiv:0803.3286.
[16] K. Haule, J. H. Shim, and G. Kotliar, arXiv:0803.1279.
[17] K. Kuroki *et al*, arXiv:0803.3325.
[18] X. Dai, Z. Fang, Y. Zhou, F. Zhang, arXiv:0803.3982.
[19] Q. Han, Y. Chen, and Z.D. Wang, arXiv:0803.4346.
[20] L. Boeri, O.V. Dolgov, and A.A. Golubov, arXiv:0803.2703.

[21] L. Shan *et al*, arXiv:0803.2405.
[22] G. Mu *et al*, arXiv:0803.0928.
[23] G. E. Volovik, JETP Lett. **58**, 469 (1993).
[24] G. E. Volovik, unpublished; in K. A. Moler *et al*, J. Phys. Chem. Solids **56**, 1899 (1995).
[25] I. Vekhter, P. J. Hirschfeld, J. P. Carbotte, and E. J. Nicol, Phys. Rev. B **59**, R9023 (1999).
[26] Y. Matsuda, K. Izawa, and I. Vekhter, J. Phys.: Condens. Matter **18**, R705 (2006).
[27] S. Raghu, X. Qi, C. Liu, D.J. Scalapino, and S.-C. Zhang, private communication.
[28] K. Deguchi, Z.Q. Mao, H. Yaguchi, and Y. Maeno, Phys. Rev. Lett. **92**, 047002 (2004).